Supplementary Information for

Patterned photonic crystals for hiding information

Yanan Li[a,b], Xue Zhou[a,b], Qiang Yang[a,b], Yudong Li[a,b], Wenbo Li[a,b], Huizeng Li[a,b], Shuoran Chen[c], Mingzhu Li[a]* and Yanlin Song[a]*

[a]Key Laboratory of Green Printing, Institute of Chemistry, Chinese Academy of Sciences (ICCAS), Beijing Engineering Research Center of Nanomaterials for Green Printing Technology, Beijing National Laboratory for Molecular Sciences (BNLMS), Beijing, 100190, P. R. China. Email: ylsong@iccas.ac.cn; or mingzhu@iccas.ac.cn

[b]University of Chinese Academy of Sciences, Beijing, 100049, P. R. China.

[c]Research Center for Green Printing Nanophotonic Materials, Suzhou University of Science and Technology, Suzhou, 215009, P. R. China.

Content

Methods Summary

Particle synthesis: Polystyrene nanospheres with monodispersed sizes are synthesized by a modified one-step emulsion polymerization method[1]. Briefly, styrene (19.0 g), acrylic acid (1.0 g) and methyl methacrylate (1.0 g) are dispersed in 80 mL water. 0~0.011 mmol emulsifier sodium dodecyl benzene sulfonate (SDBS, lower than the critical micelle concentration (CMC)) and 6.30 mmol buffer agent of ammonium bicarbonate are dissolved previously. Keep the reaction mixture at 70 ℃ for 0.5 h. The initiator is added separately by three times at different time: aqueous solution of ammonium peroxodisulfate (APS, 12 mL, 4 mL, 4 mL of 2.12 mmol), keep stirring at 80 ℃ for 1.5 h. Then increasing the temperature to 80 ℃ before the second addition of APS, and react for another 2 h. Finally, the polymerization reaction carries out at 80 ℃ for 2 h with continuous stirring for the third addition of APS solution. The dispersity of the latex spheres is no more than 0.005, determined by using a granulometer (ZetaPALS BI-90plus, Brookhaven Instrument). The resulting latex spheres were used directly without purification.

Photonic crystal pattern fabrication: 5 μL of each suspension droplet with monodispersed polystyrene nanospheres of 1.5~3%wt and surfactant of 2.5×10^{-5}wt are directly dropped by pipette on clean glass slide (contact angle 42°), and drying on hot plate at 70 ℃ for about two minutes. The pattern size and drying time depend on the liquid volume. According to the Bragg's Law:

$$m\lambda = \frac{\sqrt{6}}{3} d \sqrt{n_{eff}^2 - \sin^2\theta}$$

where m is an integer determined by the order given; λ is the wavelength of incident wave, or the stopband position; d is the particle diameter; n_{eff} is the effective refractive index; θ is the detection angle (detail provided in Supplementary S1). The different stopbands are acquired by assembling monodispersed polystyrene nanospheres with size arranging from 170 nm to 290 nm. The white dot is prepared via the same method by drying the emulsion with polydispersed nanoparticles. We use the mixture of three kinds of monodispersed nanoparticles with diameter of 360 nm, 270 nm and 180 nm in 1:1:1 mol. Other PC patterns are fabricated by dispersing emulsion on a wetting patterned substrate and drying at the same condition as the dot pattern. Photonic crystal dots on silicon, polyethylene glycol terephthalate film (PET Film), Aluminum plate and photo paper are prepared as the same method with slight adjustment of substrate temperature, particle and surfactant concentration. The profile of the deposition is measured via a stylus profilometer (MicroFigure Measuring Instrument SURFCORDER, ET-4000, Kosaka Laboratory Ltd). The SEM image is obtained by JEOL S-4800 at 5kV, 10 μA.

Photonic crystal dot coding pattern fabrication: The encoded and encrypted photonic crystal pattern are prepared as follow: Plaintext is translated into coding and encryption text in advance for designing the position of the photonic crystal code pattern. Then the emulsion that forms the corresponding stopband as the coding or encryption rules is dispersed in order on the designed coding site and drying rapidly as the same method above.

Complex photonic crystal coding pattern fabrication: Manually dispensing the emulsion on the designed hydrophilic coding area and then drying at hot plate of 70 ℃. The patterned substrate are prepared via the photolithography method[2]. Briefly, hydrophobic fluoroalkyl silane (FAS) monolayer modified clean glass slide is patterned by UV irradiation with the help of a photomask that selectively remove the FAS molecule and forms the hydrophilic area.

The stopband map measurement: The reflection spectra of the photonic crystal samples are detected by Ocean Optics (Dunedin, FL, USA) HR 4000 fiber optic UV−vis spectrometer in reflection mode, with incident light normal to the deposition surface. The angle dependent reflection spectra are acquired by the angle resolution spectrograph in the reflection mode with incident angle varying from 0 ° to 80 ° (R1 Macroscopic Angle Resolution Spectrograph, Shanghai Ideaoptics Corporation). A fine polished Al-mirror of high broadband reflection intensity in UV-visible wavelength region is used as the contrast bright source to acquire accurate reflection intensity.

S1. SEM images of ordered particle assembly in PC dots of different colors

Photonic crystals are periodic optical nanostructures in nanometer or micrometer scale that affect the motion of photons in much the same way that atomic-scale lattices affect electrons in solids, resulting similar band-gap to photons by Bragg diffraction[3-7]. The approximate relationship between bandgap position and the detection angle in closed-packed face centered cubic crystal is demonstrated by equation[8-11]:

$$m\lambda = \frac{\sqrt{6}}{3} d \sqrt{n_{eff}^2 - \sin^2\theta}$$

Where m is an integer determined by the order given;
λ is the wavelength of incident wave, or the stopband position;

d is the particle diameter, for closed-packed face centered cubic crystal from [111] face $D = \sqrt{\frac{2}{3}} d$,

where d is the diameter of the particle;

n_{eff} is the effective refractive index demonstrated by $n_{eff} = n_p f + n_s (1 - f)$, where n_p and n_s is the refractive index of particle and space medium respectively, f is the volume packing factor;
θ is the angle between the incident ray and the normal direction of the crystal plane, also the detection angle.

According to the equation, the stopband position could be manipulated by changing the periodic parameter (including particle size and space), incident angle or refractive index.

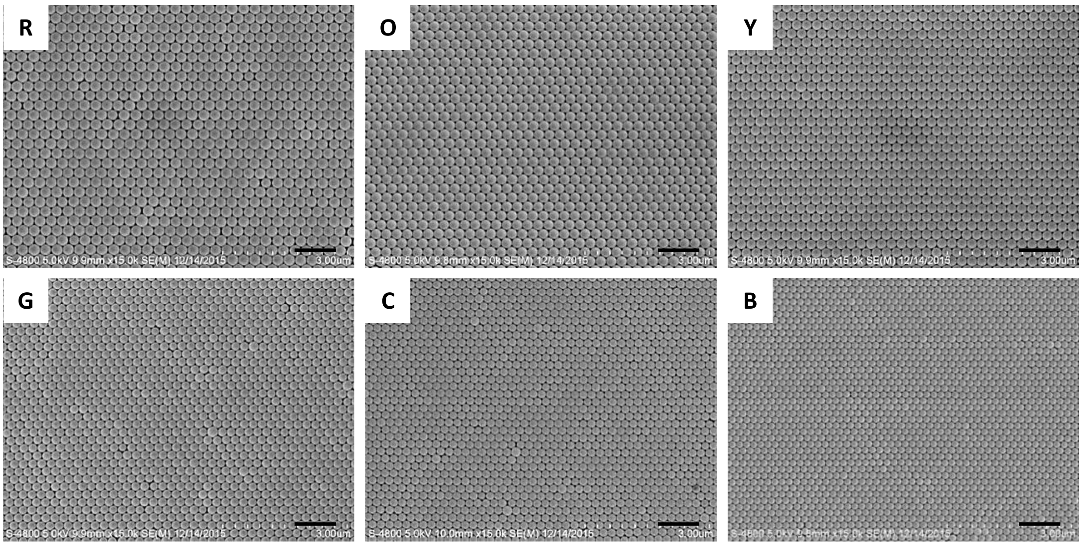

Figure S1 SEM images of ordered nanoparticle assembly in different color PC dots: Red-R, Orange-O, Yellow-Y, Green-G, Cyan-C, Blue-B. The color variation originates from the periodic change of different particle size ranging from 170 nm to 270 nm. The scale bar, 1μm.

S2. Prepared PC pattern by this drop casting method on other different substrates

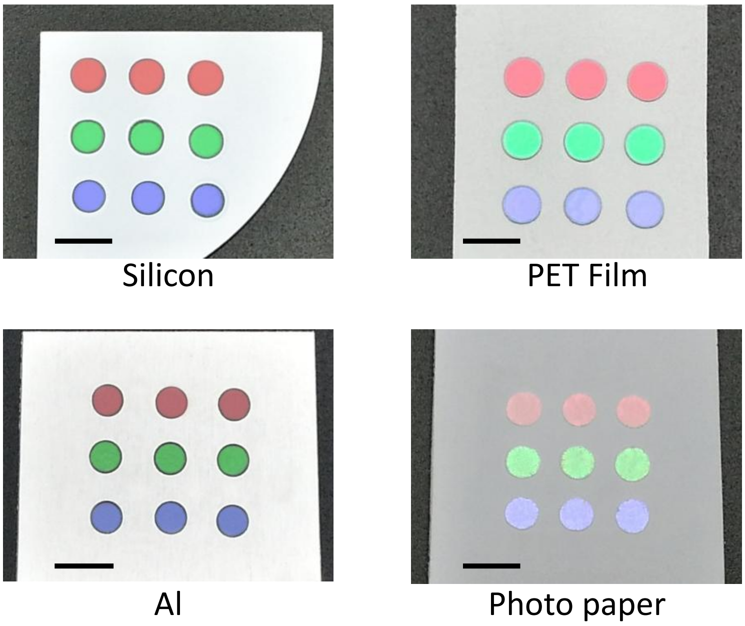

Figure S2 Photos of prepared PCP on other different substrate: silicon, polyethylene glycol terephthalate (PET) film, aluminum sheet and photo paper. The scale bar, 5 mm.

S3. Fabrication process of the substrate with wetting pattern by photolithography method

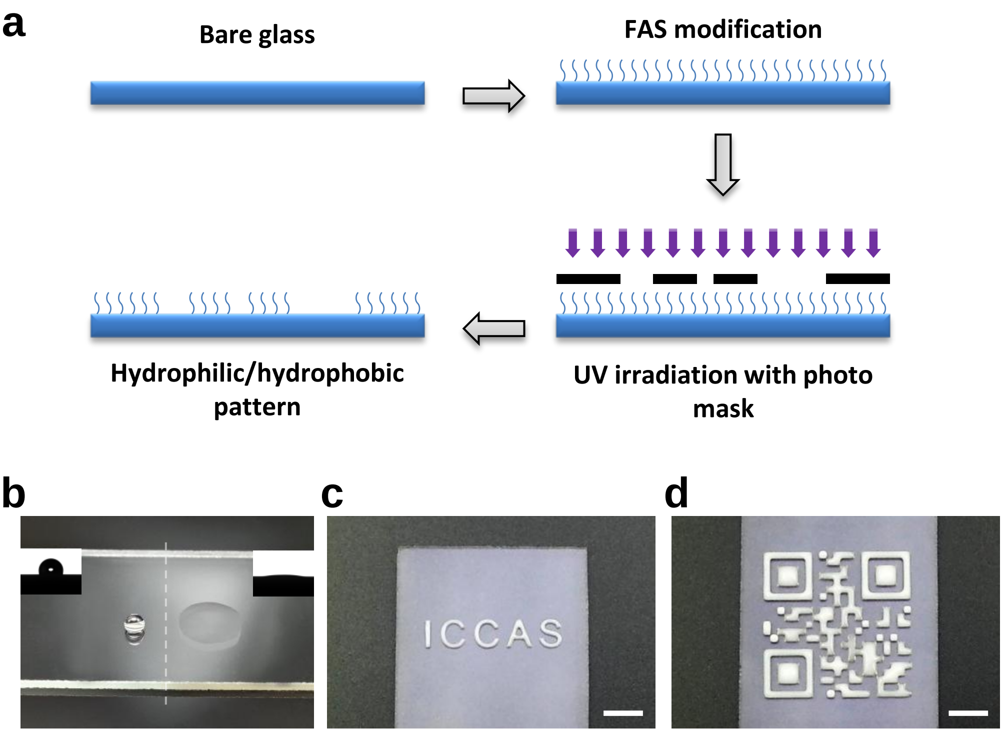

Figure S3 The preparation process of the substrate with patterned wettability by photolithography method. a, Scheme of the patterning process. **b,** Contact angle of the hydrophobic (CA=108.5±3.5°) and the hydrophilic (CA=2.7±2.5°) area respectively. **c, d,** Photos of the patterned emulsion on the wetting patterned substrate before drying. The scale bar, 5 mm in **c** and **d.**

S4. Broadband reflection spectrum of the white dot

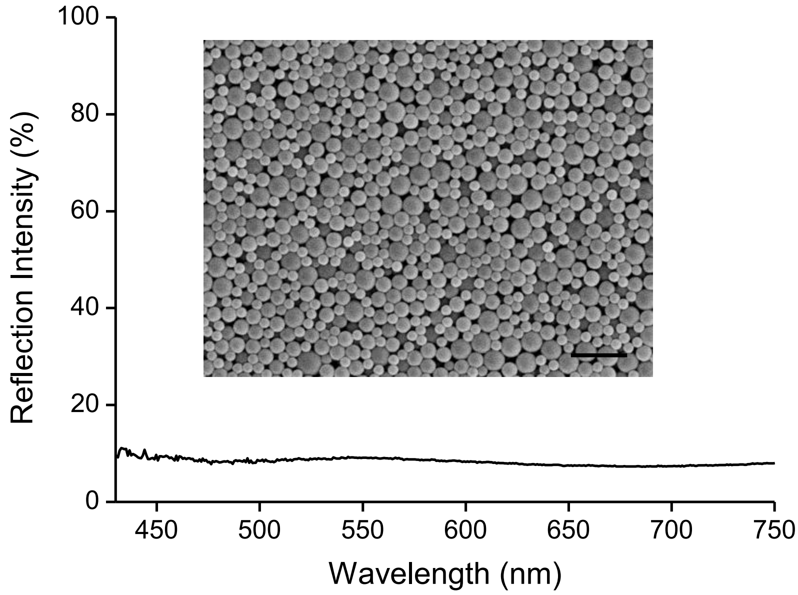

Figure S4 Broadband reflection spectrum of the white dot prepared by the deposition of polydispersed PS particles. Inset SEM image shows the amorphous arrangement of the polydispersed nanoparticles. The scale bar of the inset SEM image, 1 μm.

S5. Design of the functional sites in the coding pattern

For this 36-bit octal coding system, the decoding process of this PC coding system needs recognize and read the pattern, such as identify the orientation of the dot array, signal for start and termination. Here we use the white dot of broadband reflection as the functional site to meet these requirements. The distinct spectrum difference of these white dots could be easily identified from the dot array. The arrangement of the white dot (up-left, up- right and bottom-left, as show in the scheme below) is designed for positioning the pattern orientation according to the fundamental geometry law that two independent vectors could define a plane. After positioning the pattern orientation, we define the white dot in the corner (②) of the three orthogonal white dots as the start signal of recording. The other two white dots as the edge of the pattern and the first white dot (①) in clockwise as the end signal of recording (black dash arrow). Other seven PC dots of independent stopbands are designed as the information site for recording the information.

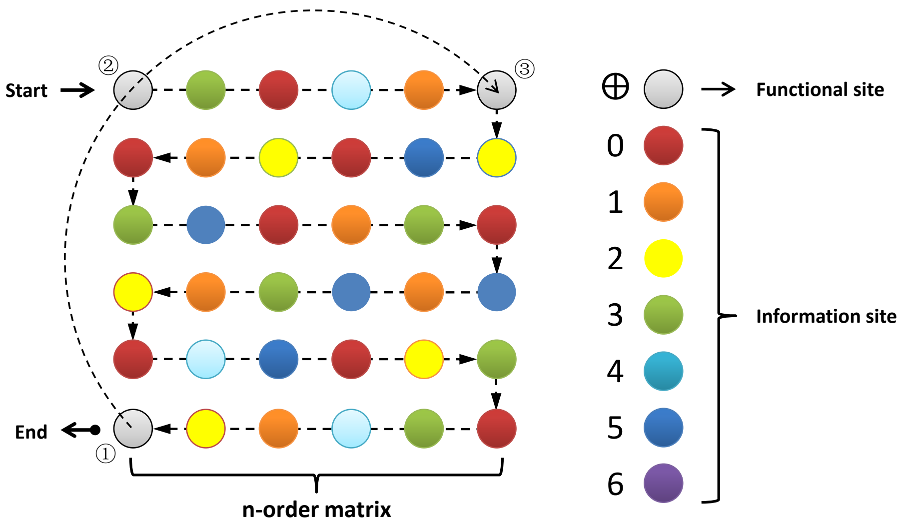

Figure S5 Demonstration of the functional sites in the coding pattern. The white dot of broadband reflection (marked as ⊕) is designed as the functional site for recognition, localization, start/termination signal; the color dot (marked as 0~6) are designed as the information sites. This one white dot and the seven color dots constitute the septenary coding system.

S6. The Modified International Morse Code

Morse code is a method to transmit text information as a series of on-off clicks, tones, lights, or anything else that can be directly understood by a skilled listener or observer without special equipment. The International Morse Code encodes the ISO basic Latin alphabet, the Arabic numerals and a small set of punctuation and procedural signals as standardized sequences of short and long signals called "dots" and "dashes", or "dits" and "dahs", as in amateur radio practice[12]. This simple and versatile coding method is widely used in secret communication or the situation that cannot communicate in the common ways. Here we modified this coding rule as the algorithm to encrypt the PC dots for information encryption and anti-counterfeiting. We presupposed two distinct structural colors of Stopband #1 and Stopband #2, such as red (659 nm) and green (534 nm) for the sake of visualization, to represent the dot and dash signal in Morse code, and single white dot as letter space, double white dots as word space. The detail of the rules is shown as follows:

1. The length of a dot is one unit → Stopband #1
2. A dash is three units→ Stopband #2
3. The space between dots and dashes signals is one unit→ dot spacing
4. The space between letters is three units → Broadband dot×1
5. The space between words is seven units → Broadband dot×2

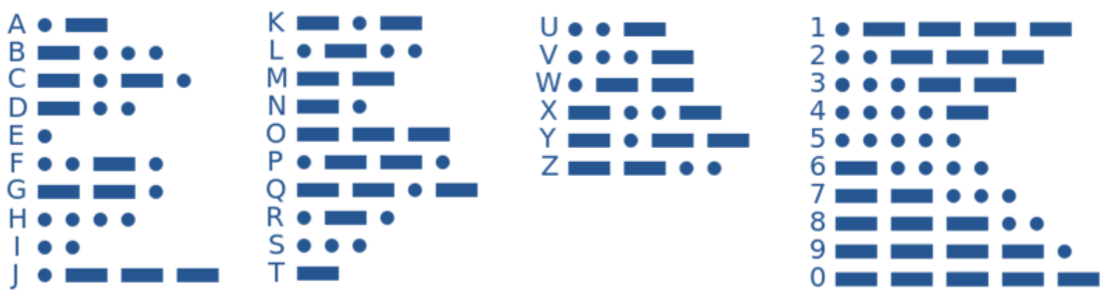

Figure S6 The rule of International Morse Code. The letters and numbers are marked as the modified rules above.

S7. Angle-dependent stopband of photonic crystals

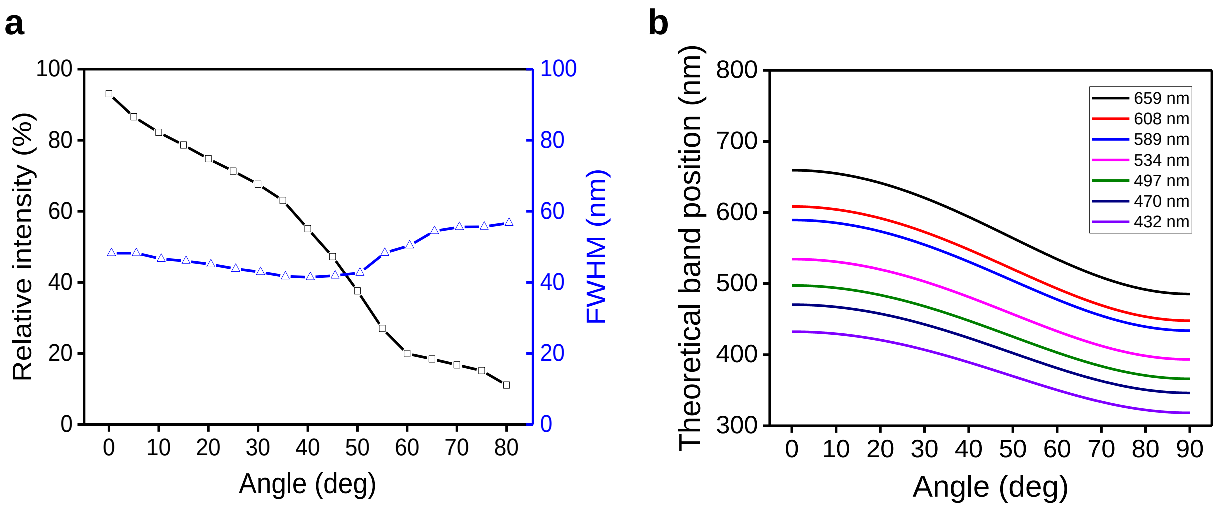

Figure S7 Angle dependent property of photonic crystal. a, Reflection intensity and full width at half maximum (FWHM) in different angle of the red PC dot. **b,** Theoretical angle dependent stopband of the seven typical structure colors.

S8. Selected stopbands for angel encryption.

a

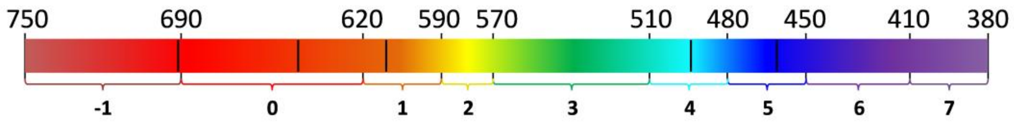

b

0º	PC dot color	white	pale red	red	orange	cyan	blue
	PC dot	○	●	●	●	●	●
	Selected band (nm)	none	689	645	611	494	461
	Signals posing	⊕	-1	0	1	4	5
30º	PC dot color	white	red	orange	yellow	blue	violet
	PC dot	○	●	●	●	●	●
	Band position (nm)	none	649	601	571	464	435
	Signals posing	⊕	0	1	2	5	6
45º	PC dot color	white	orange	yellow	green	violet	pale violet
	PC dot	○	●	●	●	●	●
	Band position (nm)	none	608	560	534	436	408
	Signals posing	⊕	1	2	3	6	7

Figure S8 Selected optical stopband for angle encryption. a, A rescaled coding table for angle encryption by dividing the visible spectrum into eight parts and marked with numbers. **b,** Table of the selected stopband and corresponding digital signal. Blue shift of the stopband induces signal displacement for angle encryption.

References

1. L. Y. Cui, Y. F. Li, J. X. Wang, E. T. Tian, X. Y. Zhang, Y. Z. Zhang, Y. L. Song and L. Jiang, *J. Mater. Chem.*, 2009, **19**, 5499.
2. H. Li, Q. Yang, G. Li, M. Li, S. Wang and Y. Song, *ACS Appl. Mater. Inter.*, 2015, **7**, 9060.
3. Photonic Crystal, https://en.wikipedia.org/wiki/Photonic_crystal).
4. J. D. Joannopoulos, P. R. Villeneuve and S. H. Fan, *Nature*, 1997, **386**, 143.
5. Colloidal_crystal, https://en.wikipedia.org/wiki/Colloidal_crystal).
6. J. P. Ge, L. He, J. Goebl and Y. D. Yin, *J. Am. Chem. Soc.*, 2009, **131**, 3484.
7. A. C. Arsenault, T. J. Clark, G. Von Freymann, L. Cademartiri, R. Sapienza, J. Bertolotti, E. Vekris, S. Wong, V. Kitaev, I. Manners, R. Z. Wang, S. John, D. Wiersma and G. A. Ozin, *Nat. Mater.*, 2006, **5**, 179.
8. K. Busch and S. John, *Phys. Rev. E*, 1998, **58**, 3896.
9. A. Richel, N. P. Johnson and D. W. McComb, *Appl. Phys. Lett.*, 2000, **76**, 1816.
10. Y. Huang, J. Zhou, B. Su, L. Shi, J. Wang, S. Chen, L. Wang, J. Zi, Y. Song and L. Jiang, *J. Am. Chem. Soc.*, 2012, **134**, 17053.
11. R. J. D. Tilley, *Colour and the optical properties of materials: an exploration of the relationship between light, the optical properties of materials and colour*, Wiley, Hoboken, N.J., 2nd edn., 2011.
12. Morse code, https://en.wikipedia.org/wiki/Morse_code).